Landscape and Urban Planning 157 (2017) 561–576

Contents lists available at ScienceDirect

Landscape and Urban Planning

journal homepage: www.elsevier.com/locate/landurbplan

Research Paper

Intense summer heat fluxes in artificial turf harm people and environment

C.Y. Jim

Department of Geography, University of Hong Kong, Pokfulam Road, Hong Kong, China

HIGHLIGHTS

- High air-cum-surface temperature of artificial turf raises concerns on player health.
- Solar & terrestrial radiation and temperature at five levels were monitored in summer.
- Artificial turf admits more solar and emits more thermal radiation than natural one.
- Artificial turf with low specific heat and moisture incurs fast heating and cooling.
- Cooler periods fit for matches were identified on sunny, cloudy and overcast days.

ARTICLE INFO

Article history:
Received 14 March 2016
Received in revised form 6 September 2016
Accepted 10 September 2016

Keywords:
Natural and artificial turf
Solar and terrestrial radiation
Radiant flux ratio
Aggregate thermal index
Energy budget tipping-point
Solar-induced thermal divergence

ABSTRACT

Artificial turf (AT) sports fields have increasingly replaced natural turf (NT). High AT material-cum-air temperature incurs heat-stress impacts on athletes, demanding better understanding of thermal regimes vis-à-vis weather conditions. Adjacent AT and NT sites in humid-tropical Hong Kong were studied. Four radiant-energy components (direct-solar, reflected-solar, sky-thermal, ground-thermal) and five temperature levels (150, 50 and 15 cm, turf-surface, substrate) were monitored in replicate, for three summer weather conditions (sunny, cloudy, overcast). Inter-site differences are attributed to lower AT albedo, admitting more shortwave and emitting more longwave radiant energy. Drastic decline in solar fluxes contrasts with terrestrial fluxes which remain intense. AT materials, with low specific heat and moisture and scanty evapotranspiration, induce fast warming and cooling with little time lag to synchronize with insolation rhythm. On sunny day, AT turf-surface, heated to 72.4 °C comparing with NT at 36.6 °C, dissipates heat by conduction and convection to near-ground air and by strong ground-thermal emission. Exceeding the heat-stress threshold most of the time, AT cools quickly from late afternoon for heat-safe use soon after sunset. On cloudy day, subdued AT heating allows earlier cooling in late afternoon. Both sites are heat-safe on overcast day. The findings can optimize game scheduling to prevent heat-related injuries.

1. Introduction

Some natural turfgrass sports fields are beset by problems in material, design, maintenance and use impact. They could suffer from chronic turf deterioration and hence degradation in site quality, with implications on player satisfaction and performance. Different management responses have been adopted to tackle the problems. The proactive measures include improving turf constitution, care, growth and durability. In contrast, the passive approach calls for notable reduction in turf wear by trimming the duration and the intensive types of use. The more drastic reaction would replace natural turf (NT) with artificial turf (AT), which has been advocated as a less costly, easier to maintain and more durable alternative.

The first-generation AT invented in the 1960s was akin to a green-colored carpet (Fleming, 2011; McNitt, 2005). Gradual evolution in material and technology has moved towards emulating the real grass in terms of appearance, feel, and playability. The present third-generation AT, emerging in the 1990s, has longer and upright fibers (or piles) which mimic linear grass leaf blades. The granular infill materials that bury the lower part of the piles mimic the mineral soil substrate of NT. The common infill substances are rubber granules or silica sand, or a mixture of both. The shockpad laid immediately below the backing sheet of the piles enhances resilience of the playing surface. Most AT fields use recycled rubber

E-mail address: hragjcy@hku.hk

http://dx.doi.org/10.1016/j.landurbplan.2016.09.012

tire shredded into small fragments for the infill and the shockpad. Usually the synthetic Styrene Butadiene Rubber (SBR) is employed, purportedly advocated as a contribution to environmental protection by giving a second lease of life or adaptive use to an otherwise waste material facing thorny disposal problems (Madison Athletic Foundation, 2011).

Five decades of AT use and studies have accumulated a rich body of knowledge on its characteristics, management and player response. The main concerns include the interface between player and surface, and between ball and surface, which were compared with NT serving as the default standard. Deviations from NT could undermine player satisfaction and performance, and may induce more frequent and serious injuries. A more critical issue is the inordinately hot AT surface which could exceed NT by 30 °C–65 °C on hot summer sunny days (Buskirk, Mclaughlin, & Loomis, 1971). The undesirable heat impacts on the comfort and health of players, especially at a surface temperature above the 45 °C heat-pain threshold, were evaluated by Kandelin, Krahenbuhl, & Schacht (1976). Subsequent studies in various cities in the temperate climatic zone and using different AT types have found similarly elevated surface temperature (Brakeman, 2004; Fresenburg, 2005; McNitt and Petrunak, 2007; Petrass, Twomey, & Harvey, 2014; Petrass, Twomey, Harvey, Otago, & LeRossignol, 2015; Sciacca, 2008; Williams and Pulley, 2002).

The relationship between some meteorological parameters and AT surface temperature was verified by Ramsey (1982), and Petrass et al. (2014) who also found an association with AT materials. The heat energy, derived from solar radiation and stored in the AT materials, could in turn warm the near-surface air mainly by conduction and convection (Aoki, Matsuda, Toyoda, 2005; Aoki, 2011; Brakeman, 2004; Kandelin et al., 1976; McNitt, 2005; Ramsey, 1982). The hot radiating surface and warmed air could raise the body temperature of players to a harmful level. In acute situations, they could suffer from heat stroke and even mortality (Aoki et al., 2005; Howe and Boden, 2007).

The ball games played under high temperature conditions could lead to heat stress and heat injury, with implications on athlete performance, health and professional lifespan (Claudio, 2008; Department of Sport & Recreation, 2011). To avoid mishaps, game scheduling has been adopted by the management to reduce the ill effects on players (Grundstein et al., 2014; Kajiwara, Ono, Nakai, Kimura, & Nozaki, 2005).

The looming climate-change impacts are accentuated in cities due to superposition of the urban heat island (UHI) effect. NT sites are important parts of the urban green infrastructure (UGI) which can provide the welcomed cool island effect. Increasing conversions of NT to AT could intensify the UHI effect and counteract the efforts to cool cities by the cost-effective and sustainable means of urban green spaces (UGS). Predicting and avoiding extremely hot periods is preferred to disruptive and unwelcomed cancellations. With climate change, more heat waves are expected in conjunction with increasing frequency and magnitude of extreme weather (Amengual et al., 2014; IPCC, 2013). The heat impacts of AT in terms of intensity and duration could be accentuated. Based on weather data and forecast in summer, days and time-periods with high risk can be avoided for practices and matches. To optimize schedule management, the magnitude of the aberrant heat regimes of artificial versus natural turf could be evaluated on selected summer days.

From a survey of the AT literature cited above, some notable knowledge gaps could be identified. As a relatively new field of study, the number of research papers is limited and the research methods are being developed progressively. Existing studies on AT microclimate concentrate on taking temperature readings in the daytime. The 24-h diurnal-cycle monitoring would have deciphered the heat exchanges in nighttime which is an integral part of the energy budget. Most studies report temperature records on the turf surface and sometimes at one height above the ground. Few would track the vertical air temperature profile at different heights as well as the turf surface and substrate. Most importantly, there is a lack of evaluation on the pertinent solar and terrestrial radiation fluxes which are the fundamental driver of the heat build-up and thermal regime of AT fields. Moreover, most studies focus on the fine-sunny weather condition, and ignore the overcast and rainy weather types. They look at one AT field without comparing it with an NT field to identify the major differences. Almost all studies were conducted in temperate climate, with few in the tropical zone. Overall, there is a lack of a detailed investigations on the holistic energetics and thermal behavior of AT, and their intimate association.

This experiment was developed to fill the above knowledge gaps, with the help of state-of-art environmental monitoring equipment especially regarding collection of accurate data on solar and terrestrial radiation. The main research questions are: (1) What are the pathways and magnitudes of heat fluxes in AT and NT under three main summer weather conditions? (2) What are the key characteristics of the thermal regime at different heights and times of the day at AT vis-a-vis NT? The study was designed to test two hypotheses: (1) The shortwave and longwave radiant-energy budget plays a key role in determining the heat fluxes of AT; and (2) The inherent physical properties of AT materials dictate its thermal regime and stress on athletes. As the study is concerned with the heat dynamics of the AT system, it concentrates squarely on the summer season. The NT field was included in the experiment as a control or a baseline to assess the thermal deviation of AT from the normal expectations of a conventional NT sports field. It is hoped that this study could generate new knowledge to improve understanding of the AT high-temperature phenomenon using a holistic radiant-energy approach.

Based on humid-tropical Hong Kong, this study assessed with the help of field experiments the heat fluxes and thermal regimes of AT vis-à-vis NT in summer. Key climatic parameters were monitored in diurnal cycles. Data of three weather types, namely sunny, cloudy and overcast days, were collected. Solar and terrestrial radiant energy components, both incoming and outgoing, were measured in conjunction with temperature at different heights, on turf surface, and in substrate. The radiant and thermal regimes of AT and NT were compared with reference to the three weather types. The thermal ambience of the two turf fields in relation to weather was ascertained.

2. Study area and methods

2.1. Experimental site

Hong Kong is situated at the northern edge of the Asian tropical zone in south China, at latitude 22°N. The regional weather is mainly regulated by the large-scale Monsoon system. It brings ample rainfall and humid condition in summer, and a cool-dry winter (Hong Kong Observatory, 2015a). The annual rainfall reaches 2400 mm, mainly dropped in the wet season extending from May to September, often associated with thunderstorms, typhoons (tropical cyclones), and heavy frontal rains. The summer temperature often exceeds 30 °C, but winter tends to be mild and seldom dropping below 10 °C. The intervening spring is warm and humid, whereas autumn is warm and dry. On sunny summer days, global solar radiation is intense, which may exceed 900 Wm^{-2} around midday to bring daily global solar radiation usually over 20 MW m^{-2} (Chong and Lee, 2015).

The weather records are indicating climate change, including rising average temperature of 0.6 °C per decade in 1985–2014, exceeding the long-term 1885–2014 average of 0.12 °C per decade (Hong Kong Observatory, 2015b; Lee, Chan, Ginn, & Wong, 2011). Meanwhile, extreme weather events for rainfall (hourly rainfall ≥100 mm, 2-hourly rainfall ≥150 mm, 3-hourly rainfall ≥200 mm) and extremely hot days (≥35 °C) have become more frequent as expressed by notably shortened return periods. The impacts on outdoor workers and athletes on hot summer days call for preventive actions. The community expects the administration to mitigate the effect of climate change which has been compounded by the aggravating UHI effect (Lo and Jim, 2015).

The exceptional compact urban development mode in Hong Kong is characterized by dense packing of high-rise buildings and roads. Due to the rugged topography and shortage of flat and easily developable land, the 7.24 million population is accommodated in merely 250 km^2 of built-up areas, occupying about a quarter of the 1108 km^2 land area (Planning Department, 2015). UGS are seriously lacking, with public urban open-space provision at merely 2.84 m^2/person, which is one of the lowest in the world for comparable large cities (Jim and Chan, 2016). The deprivation of UGS restricts opportunities for outdoor recreation with health and quality-of-life implications (Hong Kong Council of Social Service, 2014), and gravely limiting the contributions of greenery to cooling and UHI mitigation (Jim, 2015).

The experimental sites are situated at the sports center of the University of Hong Kong, at a coastal location with a high skyview factor, excellent exposure to sunlight, and high permeability to wind and ventilation (Fig. 1). It has four rectangular sports fields, three of which have been converted to artificial turf. The study evaluated the microclimate of AT which was compared with NT serving as the baseline. The experimental design demands adjacency of the two fields to ensure that they are exposed to similar solar radiation and general weather conditions. The fields are designed for soccer and hockey games, and they meet the guidelines stipulated by the relevant international bodies, namely the International Federation of Football Associations (FIFA, 2015) and International Hockey Federation (FIH, 2014).

The NT site is planted with a cultivar of Bermudagrass (*Cynodon dactylon*) with a fine texture and tolerance of relatively cool winter weather. It can remain green and robust through the cool-dry winter months, and grows vigorously in the hot-humid summer. The substrate is a prepared soil mix composed of local well-weathered granitic material, with the topsoil enriched with organic matter (Jim, 1996). Drainage is facilitated by surface crowning and subsoil drain pipes. An automatic sprinkler irrigation system provides supplementary watering.

A third-generation product was installed at the AT field (Fig. 2). The synthetic grass leaves are composed of 35-mm long green-colored polyethylene mono-filament fibers. The AT pile is held upright by granular infill, including an upper 8-mm layer of rubber granules made of shredded recycled rubber tires, and a lower 10-mm layer of quartz sand. The fibers are weaved into a double backing sheet made of polypropylene and polyester and fixed to it by an adhesive coating. The backing sheet is perforated to allow water to drain downwards. The above materials are underlain by a 25-mm recycled rubber-pellet shockpad to improve resilience of the playing surface. Below the shockpad, a 65-mm layer of no-fines concrete offers the firm and flat base that allows free drainage. The site soil lying below it serves as the sub-base which is equipped with corrugated plastic drain pipes.

2.2. Experimental design

The two turf sites were given the same experimental treatments. Each site was equipped with two similar microclimatic monitoring stations (Fig. 3). Each station contained the following research-grade environmental sensors with weather-proof design

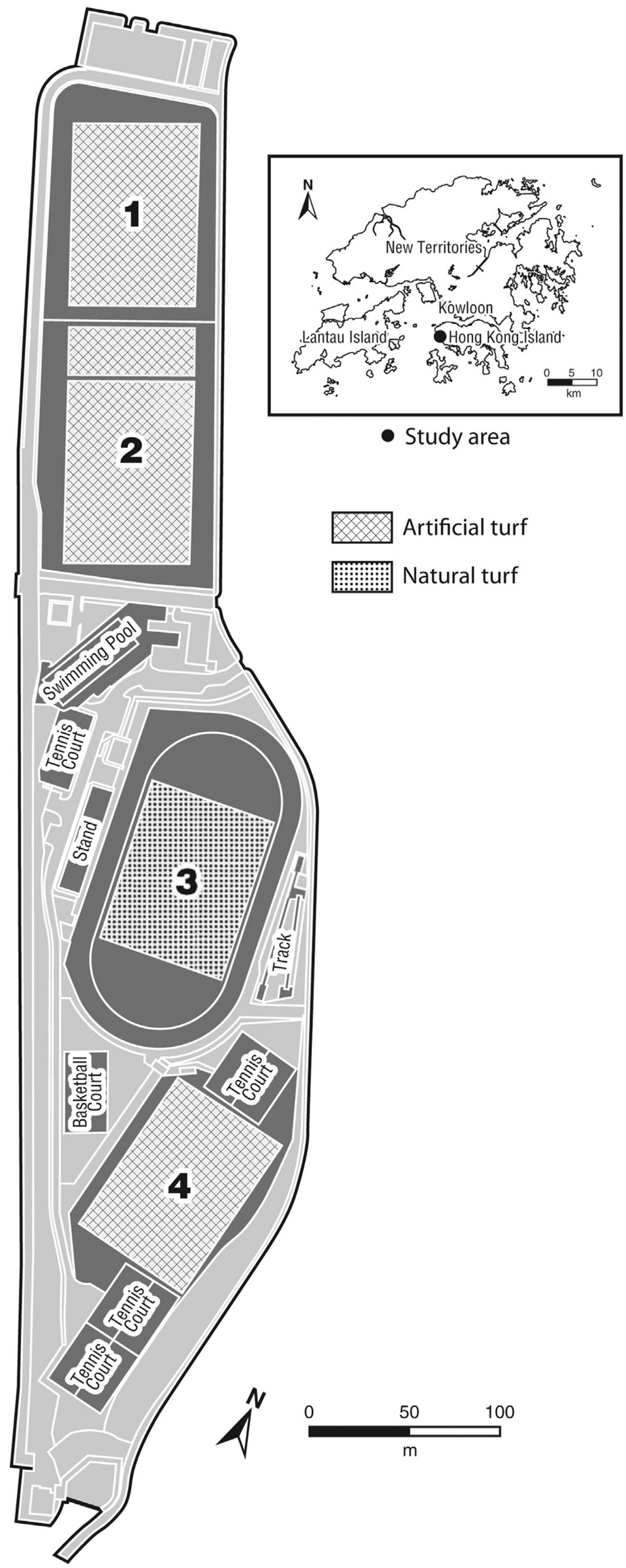

Fig. 1. Location of the study area which is the sports fields of the University of Hong Kong situated at a western coastal strip of Hong Kong Island as indicated by the inset map. Field 2 artificial turf and adjacent field 3 natural turf were chosen for the microclimatic monitoring.

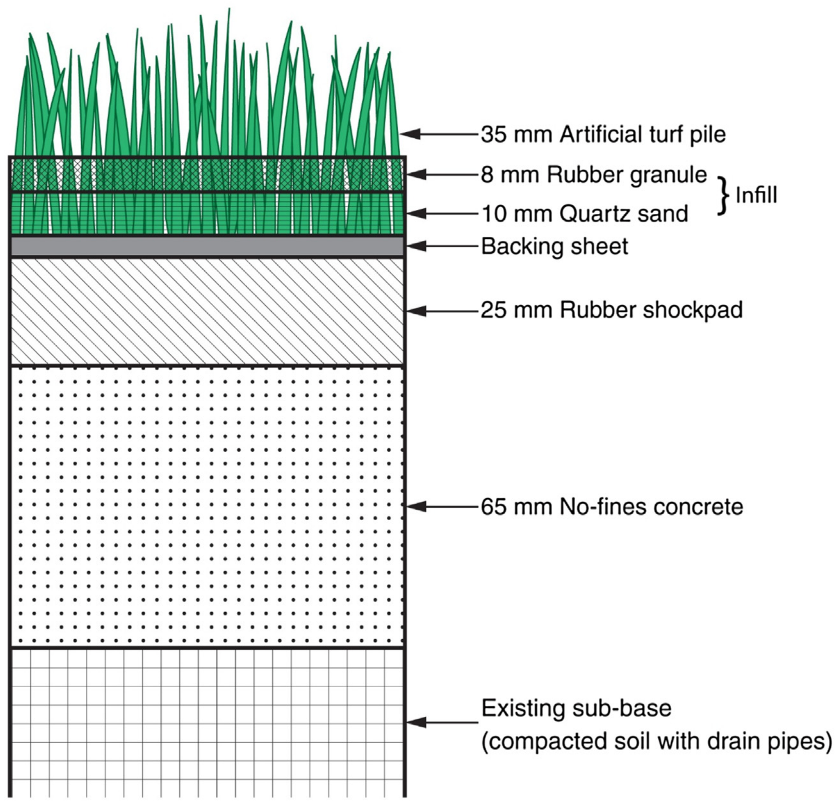

Fig. 2. Cross-sectional view of the third-generation artificial turf at the study site showing the vertical sequence of different material layers.

Table 1
Environmental monitoring sensors used in the field experiment to measure temperature, humidity, radiation, wind and rainfall at the natural and artificial turf sites.

Sensor and installation position[a]	Sensor type	Accuracy & unit	Brand, model and manufacturer location[b]
(a) Temperature:			
Air 15, 50 and 150 cm	Thermister	±0.2 °C	Hobo S-THB, Bourne, MA, USA
Turf surface	Infrared radiometer	±0.2 °C	Apogee SI-111, Logan, UT, USA
Substrate at 6 mm depth	Pt100	±0.4 °C	Lufft 8160.TF, Fellbach, Germany
(b) Relative humidity:			
Air 15, 50 and 150 cm	RH sensor	±2.5%	Hobo S-THB, Bourne, MA, USA
(c) Radiation (at 160 cm):			
Solar incoming and outgoing	Net radiometer	<5% $W\,m^{-2}$	Kipp & Zonen CNR4, Delft, Netherlands
Terrestrial incoming and outgoing	ditto	<5% $W\,m^{-2}$	ditto
(d) Weather station[c] (at 160 cm):			
Wind speed and direction	Cup anemometer	±0.5 m/s	Hobo S-WCA, Bourne, MA, USA
Rain gauge	Tipping bucket	±1.0% mm	Hobo S-RGB, Bourne, MA, USA

[a] Each turf site was equipped with two monitoring stations including the same set of sensors to acquire duplicate data.
[b] The Lufft Opus 200 and 208 data loggers (Fellbach, Germany) were synchronized and programmed to acquire data at 15-min interval.
[c] Wind and rain measurements were taken at one of the two monitoring stations at each turf site.

for outdoor use. The manufacturer and accuracy information of the sensors are summarized in Table 1:

(a) Two pyranometers, covering the shortwave spectral range of 300–2800 nm, pointing upwards and downwards to measure respectively direct and reflected solar radiation (Kipp and Zonen, 2009).
(b) Two pyrgeometer with longwave spectral range of 4500–40,000 nm, pointing upwards and downwards to measure respectively sky thermal and ground thermal radiant energy (Kipp and Zonen, 2009).
(c) The above four sensors were fitted by the manufacturer in a four-in-one net radiometer design with a built-in temperature sensor for temperature correction of the measured data. The four readings allowed establishment of the radiant energy budget for both solar and terrestrial radiation at the study sites. The overall net radiation for each site could be computed.
(d) Air temperature at 150, 50 and 15 cm from the ground using thermister probes equipped with radiation shield.
(e) Turf surface temperature using a non-contact infrared radiometer.
(f) Substrate temperature using a Pt100 soil temperature probe buried at 6 mm depth.
(g) Relative humidity at 150, 50 and 15 cm from the ground using the capacitive type of sensors.
(h) Wind speed and direction at 160 cm height using a cup anemometer and a wind vane.
(i) Rainfall at 160 cm height using a tipping-bucket rain gauge.

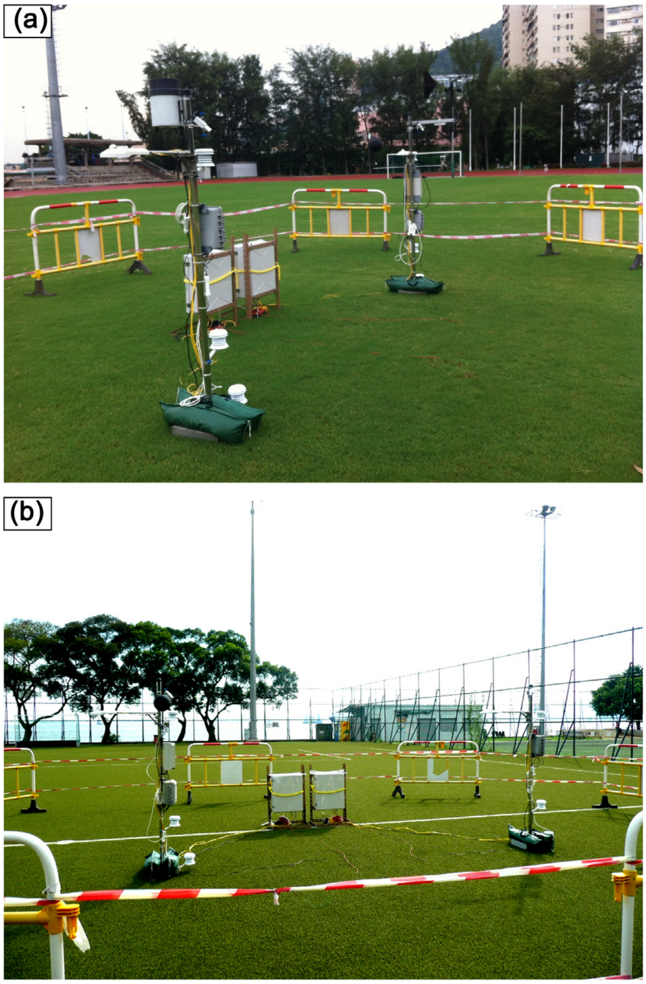

Fig. 3. The replicate microclimatic sensors and dataloggers installed at two fields at the sports center of the University of Hong Kong: (a) Natural turf (NT); and (b) Artificial turf (AT).

(j) The monitoring data were acquired at 15-min intervals and stored in data loggers for periodic transfer to a notebook computer.

The study was conducted in summer 2014. As the university sports center was heavily used throughout the year, especially in summer, the request to have continuous monitoring for two months could not be approved. Instead, the manager permitted booking only of some assigned two-day slots both turf fields in July to August, which are the hottest months. The intention was to capture three types of summer weather conditions, namely sunny, cloudy and overcast. The captured days have weather conditions that fall within the average conditions based on the 30-year weather normals of the local weather station (Hong Kong Observatory, 2016). Replication to improve data reliability was achieved in two ways. Firstly, two microclimatic stations were installed at each turf site collecting two sets of data concurrently. Secondly, more than one day of data were collected for each weather type. As the data of both replications were very similar, this paper has chosen to present one set rather than using averages.

Two radiant flux indices were devised to characterize the amount and relative proportion of radiation components fluxing at the turf sites:

(a) Radiant flux index (RFI) = Direct solar radiation + Reflected solar radiation + Sky thermal radiation + Ground thermal radiation. It indicates the total amount of solar and terrestrial radiation entering and leaving a turf site on a daily basis.
(b) Radiant flux ratio (RFR) = (Direct solar radiation + Reflected solar radiation)/(Sky thermal radiation + Ground thermal radiation). It compares the solar radiant flux with the terrestrial radiant flux on a daily basis, indicating the relative magnitude of the two radiant components.

In addition, two thermal indices were developed to characterize the relative magnitude of the thermal energy content at the two sites:

(a) Aggregate thermal index (ATI) = $\Sigma(x - 30)/32$, using the top 32 highest temperature values recorded within a sample day (x) and 30 °C as threshold above which the temperature is considered as high for humid-tropical summer.
(b) Site ATI = Average of the five ATI values at the five measurement positions.

3. Results and discussion

3.1. Sampled days for three weather types

The microclimatic data were evaluated to select suitable days to represent sunny, cloudy and overcast conditions. The key weather parameters of the three chosen days in comparison with the urban weather station records are given in Table 2. At each site, the two replicate monitoring stations yielded similar results. Data from one station was used in the analysis; no attempt was made to average the two data sets.

Daily solar radiation input was the overarching factor of weather differentiation, with sunny day shooting above 20 MW m^{-2} which is about two-third of the maximum value received by the Earth (Gates, 2003), cloudy somewhat above 10 MW m^{-2}, and overcast below 10 MW m^{-2} (Table 2). The approximate relativity of incident solar energy of the three weather scenarios was 100:50:25. The government's main weather station is situated in the city core, originally with an urban fringe environs when it was established in 1883, which has since been surrounded by high-density urban sprawl. Wrapped around by built-up areas, the location registered less solar radiation and bright sunshine duration and lower temperatures than the well-exposed study sites.

The temperature records showed differences by weather type, with progressively lower maximum and minimum temperatures and narrower diurnal range in response to reduced solar radiation input (Table 2). Relative humidity (RH) indicated an inverse relationship with temperature, with higher temperature associated with lower RH. Sunny and cloudy days had meager rainfall respectively of 3.4 mm and 0.8 mm, whereas overcast had 7.0 mm.

3.2. Radiant flux on sunny day

On sunny day, the predominantly incoming solar irradiance had a small reflectance fraction (Fig. 4). Direct solar radiation received at NT was slightly higher than AT, respectively at 24.49 and 23.92 MW m^{-2} (Table 3). They differed mainly by reflected solar radiation, with three times higher albedo at NT reflecting 4.61 MW m^{-2} versus merely 1.52 MW m^{-2} at AT. Consequently, AT received 2.52 MW m^{-2} more net solar radiation than NT.

Terrestrial radiation contributed a large proportion of the radiant energy fluxes at both sites. It had considerably higher incoming and outgoing fluxes than solar radiation, bringing small outgoing net radiation (Fig. 4). The sky thermal radiation records at NT and AT were similar at above 38 MW m^{-2} (Table 3). Sky thermal radiation streamed down continuously in the 24-h cycle, with its

Table 2
Main weather data of the three sampled days with different weather conditions, respectively sunny, cloudy and overcast.

Location	Notation	Sample date (yyyymmdd)	Weather type	Solar radiation (MWm^{-2})[a]	Bright sunshine duration (h)[b]	Temperature[c]			Relative humidity (mean & range, %)	Rainfall (mm)
						Maximum (°C)	Minimum (°C)	Range (°C)		
Study site	SD	20140705	Sunny	24.49	9.8	34.4	28.3	6.1	80 (69–91)	3.4
Weather station[d]				23.97	9.9	33.8	28.9	4.9	76 (65–84)	1.5
Study site	CD	20140805	Cloudy	13.24	9.8	32.3	28.2	4.1	83 (73–88)	0.8
Weather station[d]				10.69	2.0	30.7	27.3	3.4	86 (78–96)	21.1
Study site	OD	20140707	Overcast	6.48	4.5	30.5	27.7	2.8	87 (78–92)	7.0
Weather station[d]				6.84	0.9	30.3	26.9	3.4	84 (77–91)	5.5

[a] Aggregate solar radiation received on the sampled day.
[b] Bright sunshine has an intensity ≥120 $W m^{-2}$.
[c] Air temperature taken at 1.5 m height at the natural turf site.
[d] The government's main weather station is situated on a small hill surrounded by dense built-up area.

Table 3
Components of the radiant energy budget by solar and terrestrial radiation on three weather-type days at natural and artificial turf sites.

Weather type[a]	Turf type[b]	Component of radiant energy budget (MWm^{-2})							Radiant flux index[c]	Radiant flux ratio[d]
		Direct solar radiation	Reflected solar radiation	Net Solar Radiation	Sky thermal radiation	Ground thermal radiation	Net thermal radiation	Net radiation		
Daily value:										
SD	NT	24.49	4.61	19.88	38.42	42.69	−4.27	15.61	110.21	0.36
	AT	23.92	1.52	22.40	38.81	47.08	−8.27	14.13	111.33	0.30
	NT-AT	0.57	3.09	−2.52	−0.40	−4.39	3.99	1.48	−1.12	0.06
CD	NT	13.24	3.08	10.16	38.76	41.57	−2.82	7.34	96.65	0.20
	AT	13.02	0.95	12.07	39.02	43.39	−4.38	7.69	96.38	0.17
	NT-AT	0.22	2.13	−1.91	−0.26	−1.82	1.56	−0.35	0.28	0.03
OD	NT	6.48	1.52	4.96	39.00	41.06	−2.06	2.90	88.06	0.10
	AT	6.05	0.59	5.46	39.05	41.70	−2.65	2.81	87.39	0.08
	NT-AT	0.43	0.93	−0.51	−0.05	−0.64	0.59	0.08	0.66	0.02
Daily difference:										
SD-CD	NT	11.25	1.53	9.72	−0.34	1.12	−1.46	8.27	13.56	0.16
	AT	10.90	0.57	10.33	−0.20	3.69	−3.89	6.44	14.96	0.13
SD-OD	NT	18.02	3.09	14.93	−0.58	1.63	−2.21	12.71	22.15	0.26
	AT	17.87	0.93	16.93	−0.24	5.38	−5.62	11.32	23.94	0.21
CD-OD	NT	6.76	1.56	5.20	−0.24	0.51	−0.75	4.45	8.59	0.10
	AT	6.97	0.36	6.61	−0.04	1.69	−1.73	4.88	8.98	0.09

[a] The three weather types are: SD for sunny, CD for cloudy, and OD for overcast. Their key weather parameters are summarized in Table 1.
[b] The two turf sites are: NT for natural turf, and AT for artificial turf.
[c] Radiant flux index = Direct solar + Reflected solar + Sky thermal + Ground thermal.
[d] Radiant flux ratio = (Direct solar + Reflected solar)/(Sky thermal + Ground thermal).

daily total exceeding direct solar radiation by a significant margin. Ground thermal radiation was higher than sky thermal radiation at both sites. Receiving the combined inputs of direct solar and sky thermal radiation, ground thermal radiation or terrestrial re-radiation operated continuously throughout the day to dominate the radiant environment. Absorbing more direct solar radiation, AT in turn emitted more ground thermal radiation than NT, being 47.08 $MW m^{-2}$ versus 42.69 $MW m^{-2}$. Thus the net thermal radiation of AT was 3.99 $MW m^{-2}$ higher than NT.

AT admitted more solar radiation and emitted more terrestrial radiation, bringing more total radiant flux than NT. The sensible heat flux at AT was also higher due to thermal transfer from hot synthetic turf materials by conduction and convection to near-ground air. In daytime, AT emitted considerably more longwave radiation than NT, whereas in nighttime the emissions were similar (Fig. 4b). The nocturnal similarity in ground thermal emission implied that AT was cooled rapidly after sunset to restrict lingering thermal effect in nighttime. Thus the differences in terrestrial radiant fluxes occurred mainly in daytime when the fields were more actively used. In daytime, players on the AT field are exposed to high levels of thermal radiation.

The RFI on sunny day stayed high at 110 at both sites (Table 3). The RFR indicated that about one third of the flux was contributed by solar radiation. Both sunny-day values were the highest amongst the three weather scenarios. For both sites, the solar fraction surplus was approximately equal to the site net radiation gain, and the terrestrial fraction experienced net loss due to ground thermal exceeding sky thermal radiation. The lower RFR at AT implied a radiant regime with more terrestrial radiation. The overall net incoming radiation at both sites was significant and contributed mainly by solar radiation (Fig. 4). At nighttime, outgoing net thermal radiation had small magnitude. Both sites experienced notable energy accretion on the sunny day.

3.3. Radiant flux on cloudy day

On cloudy day, solar radiation contributed relatively less to the total radiant energy fluxes at both sites (Fig. 5). Direct solar radiation received at both sites was similar at somewhat above 13 $MW m^{-2}$ which was considerably below the sunny day (Table 3). However, they diverged by reflected solar radiation, with 3.08 $MW m^{-2}$ at NT which was over three times of 0.95 $MW m^{-2}$ at AT. Cloudy day albedo was higher than sunny day at NT, whereas it remained similarly low at AT, which admitted more net solar radiation.

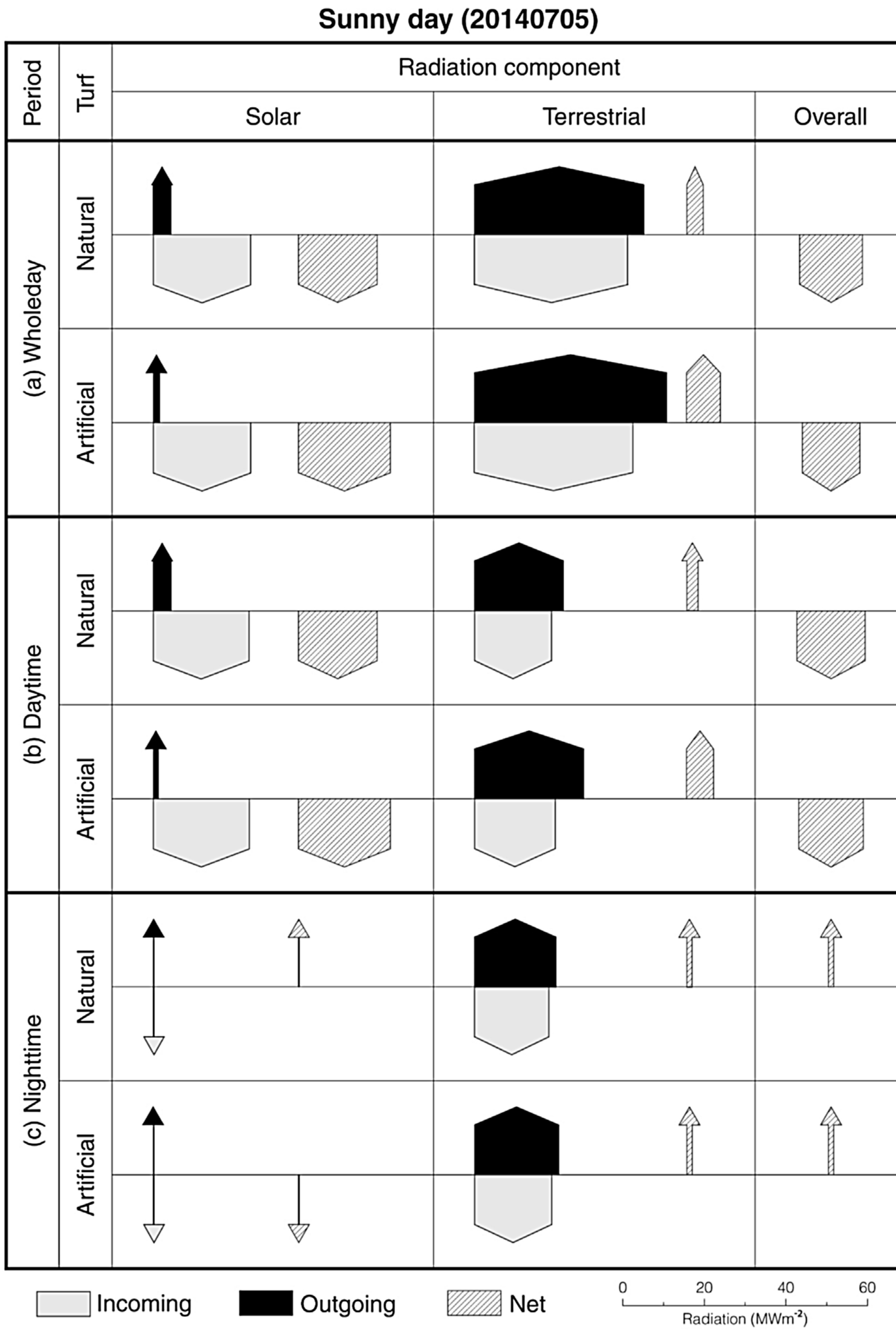

Fig. 4. The radiant energy fluxes at the natural and artificial turf sites on the sunny day (SD) in: (a) Wholeday; (b) Daytime; and (c) Nighttime.

Despite reduced direct solar radiation, sky thermal radiation on cloudy day was comparable to sunny day, with both sites receiving similar inputs. Ground thermal radiation dropped somewhat below sunny day, with AT maintaining a slightly higher level than NT. Ground thermal loss in daytime exceeded nighttime at AT, but less so than sunny day (Fig. 5b). Similar to sunny day, at AT more solar radiation gain was offset by more terrestrial loss. As AT released more of its stored heat than NT, its net thermal radiation is 1.56 MW m^{-2} higher.

Despite reduced solar radiation input, the two sites differed by lower reflectivity and higher ground thermal radiation at AT. The radiant and sensible energy budgets at AT had more fluxes than NT. The higher thermal fluxes at AT occurred mainly in daytime, during which players are exposed to the thermal impacts (Fig. 5).

The RFI on cloudy day dropped down to around 96 for both sites, mainly due to trimmed direct solar input (Table 3). The RFR of 0.20 for NT and 0.17 for AT was notably below sunny day. Again, AT was more affected by a stronger terrestrial component than NT.

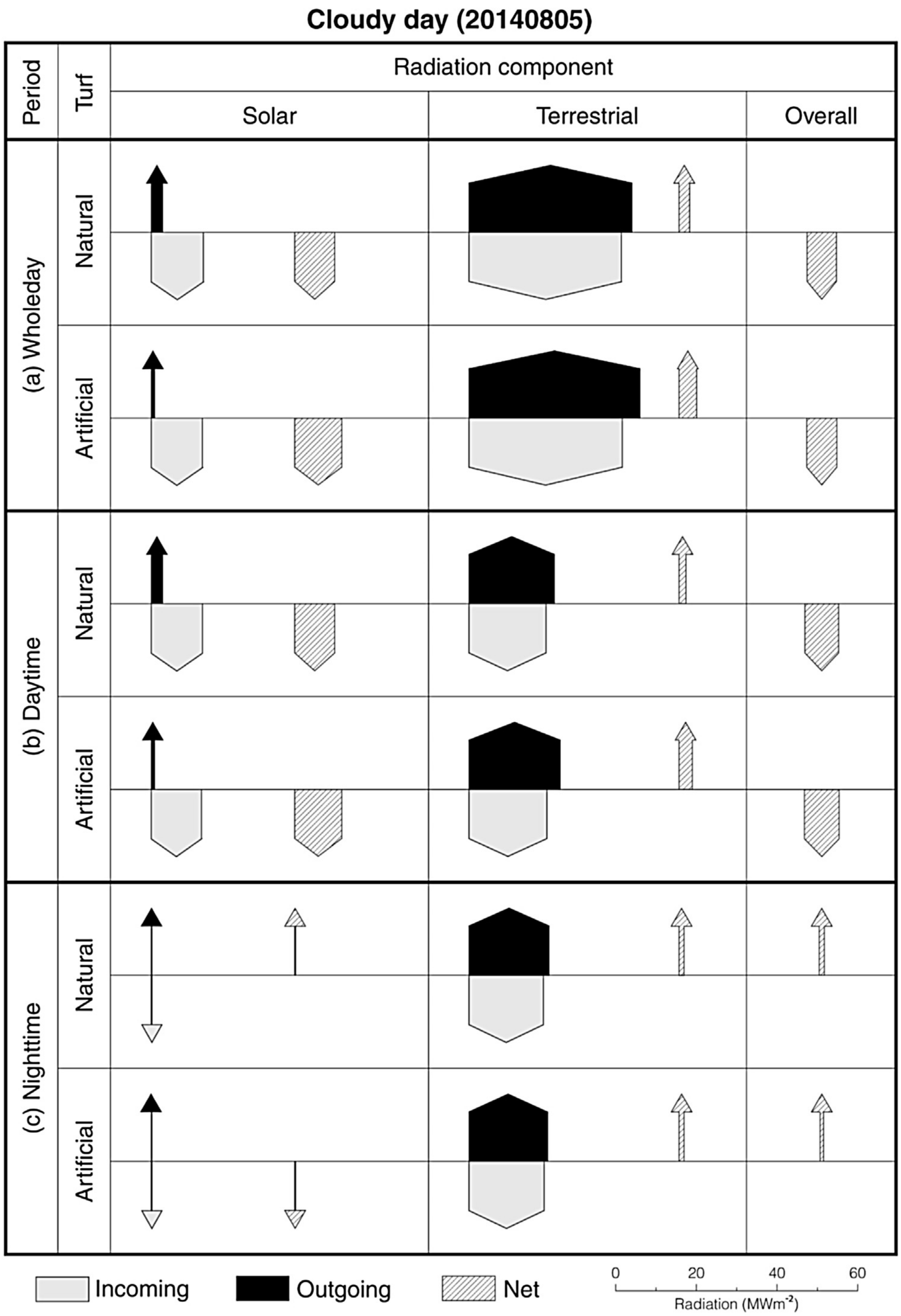

Fig. 5. The radiant energy fluxes at the natural and artificial turf sites on the cloudy day (CD) in: (a) Wholeday; (b) Daytime; and (c) Nighttime.

3.4. Radiant flux on overcast day

On overcast day, solar radiation fluxes shrank considerably whereas terrestrial radiation fluxes remained rather high and similar to cloudy day (Fig. 6). Direct solar radiation input dropped down to around 6 MW m^{-2} at both sites (Table 3). Despite the subdued solar radiation input, the reflectivity differential between NT and AT stayed similar to cloudy day. Reflected solar radiation at AT was still 0.93 MW m^{-2} lower than NT despite the reduced solar radiation input.

Sky thermal radiation on overcast day was slightly higher than sunny and cloudy days, shooting just above 39 MW m^{-2}. Ground thermal radiation was not dampened by the overcast condition, as it was only slightly lower than cloudy day. However, the difference between the two sites was depressed, with AT merely 0.64 MW m^{-2} higher than NT. The net thermal radiation of the two fields tended to converge, dropping down to merely around 3 MW m^{-2}.The reduced solar radiation input effectively suppressed the thermal differences between the two sites. Players in daytime continued to be washed by considerable thermal radiation (Fig. 6). However, unlike sunny and cloudy days, in daytime AT did not experience notably more thermal energy fluxes than NT.

The RFI at around 88 at both sites fell below cloudy day by about 9 units (Table 3). The RFR sank down to 0.10 and 0.08, indicat-

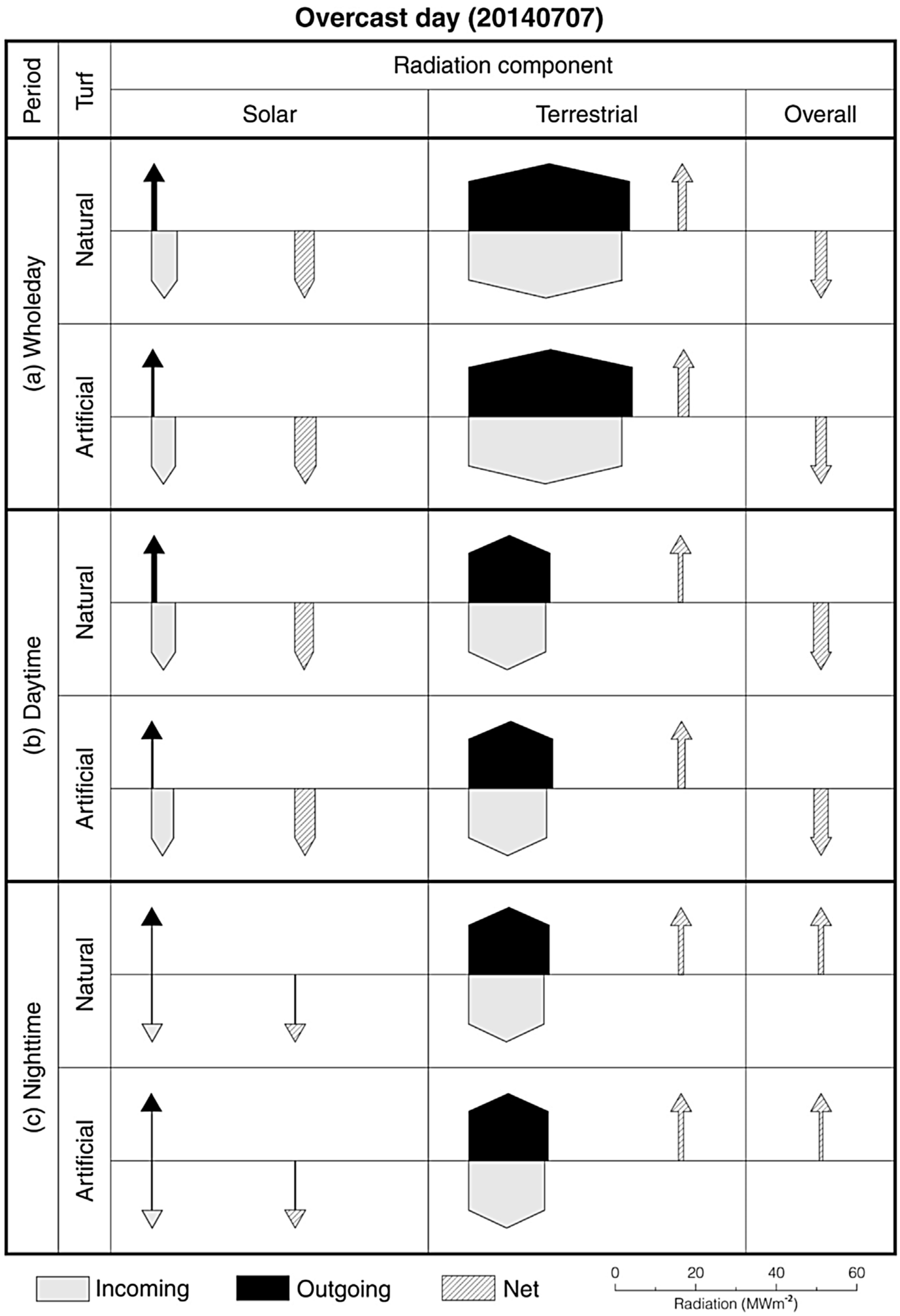

Fig. 6. The radiant energy fluxes at the natural and artificial turf sites on the overcast day (OD) in: (a) Wholeday; (b) Daytime; and (c) Nighttime.

ing strong influence of terrestrial radiation. Despite shrinking of solar radiation components, terrestrial radiant flux remained quite rigorous to dominate the radiant energy budget.

3.5. Temperature profile on sunny day

On sunny day at 0800 h, NT and AT temperatures were similar at different heights, with AT only slightly warmer at turf surface (Fig. 7a). As early as 1000 h, AT turf surface shot up to 54.5 °C compared with merely 32.5 °C at NT (Fig. 7b). At AT, the moderate morning insolation could heat up rather quickly the surface material early in the day. Conduction and convection transferred the heat stored in AT material to warm adjacent substrate (45.0 °C) and 15-cm air (38.2 °C). The warming effect could be felt at 150 cm which was 2.9 °C warmer than NT.

By noon, AT turf surface temperature peaked at 72.4 °C indicating swift thermal response to peak solar radiation input with little time lag (Fig. 7c). The stored heat was transmitted effectively mainly by conduction downwards to warm substrate to 70.4 °C. The similarity in material temperature indicated efficient heat transfer from surface to subsurface rubber-infill materials. Air temperature was lifted to 42.5 °C at 15 cm, and 36.9 °C at 50 cm. Meanwhile, NT temperature was only raised a few degrees higher than ambience

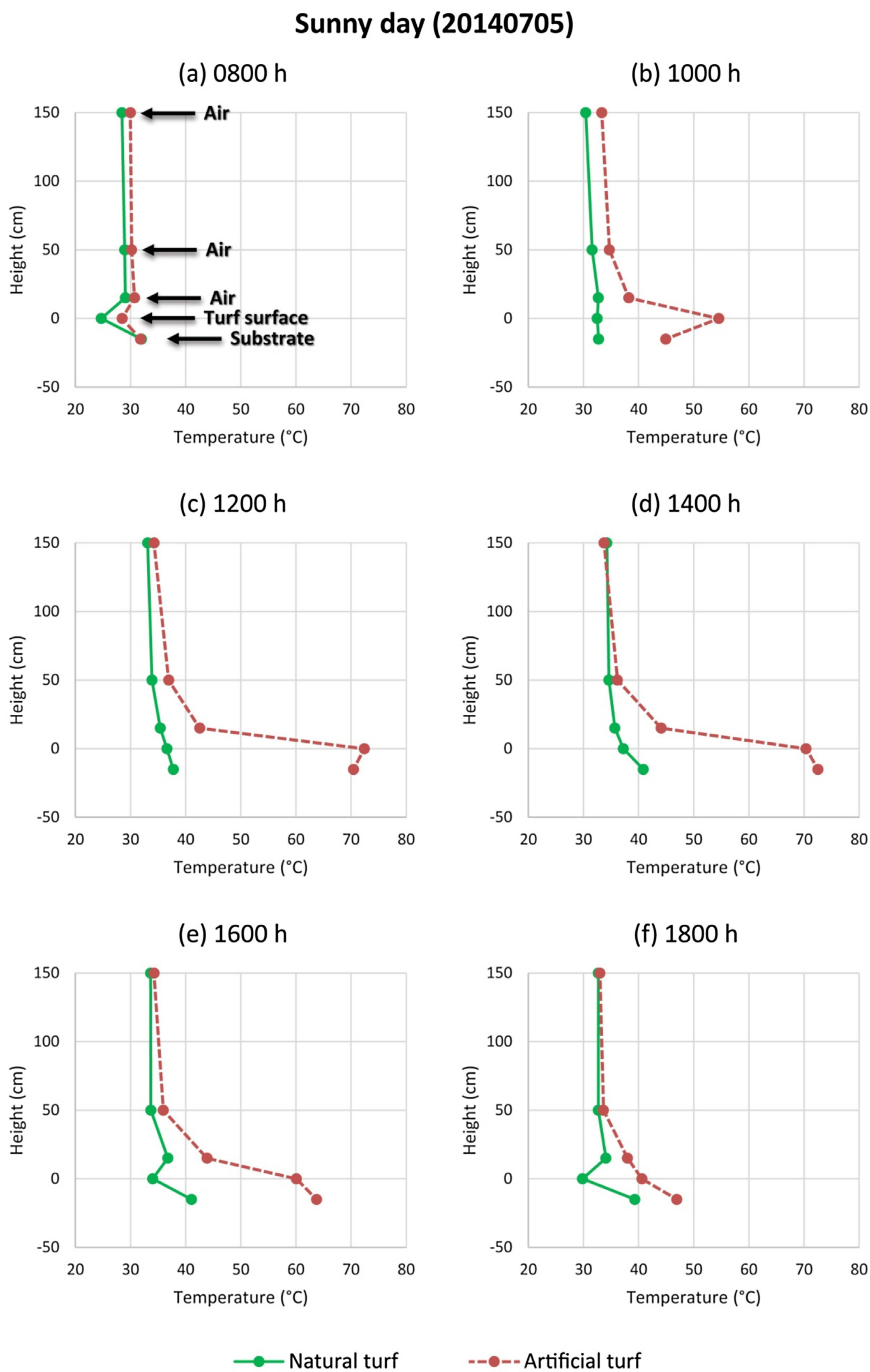

Fig. 7. Vertical temperature profiles from 150 cm height to substrate at six times on the sunny day (SD) comparing natural and artificial turf sites.

denoted by 150 cm (33.0 °C), with maximum temperature attained in substrate (37.8 °C) which was slightly warmer than turf surface (36.6 °C).

At 1400 h, AT substrate recorded the highest temperature at 72.5 °C to surpass turf surface at 70.4 °C. At 15 cm, air temperature continued to rise to 44.1 °C (Fig. 7d). At 50 cm and 150 cm, however, air temperature began to drop slightly. In comparison, NT temperatures continued to rise slightly at all five levels. Its turf surface attained the daily peak (37.2 °C), indicating a time lag in relation to solar-input peak. The NT substrate was cooler than AT by 33.2 °C, and turf surface by 31.7 °C.

At 1600 h, solar radiation input began to wane, leading to fast cooling of AT turf surface to 60.1 °C and substrate to 63.7 °C. In tandem, air temperatures at 15 cm and 50 cm also dropped slightly (Fig. 7e). At NT, substrate temperature continued to rise to the daily maximum of 41.0 °C. This result indicated establishment of the *thermal-mass effect* due to the high specific heat of soil moisture leading to *thermal inertia*, hence delayed peak temperature and sustained high temperature.

At 1800 h, close to sunset, drastic cooling occurred at AT turf surface and substrate, bringing notable drop of respectively 19.5 °C and 16.8 °C in comparison with 1600 h (Fig. 7f). The prompt temperature response to dwindling solar radiation input echoed poor *heat storage capacity* of AT materials. At NT, substrate cooled slower than turf surface, suggesting the operation of thermal inertia in the moist soil material. Air temperatures at 150 cm and 50 cm of the two sites nearly converged. Rapid cooling of AT material and air in late afternoon implied that the field experienced a plunge in heat-stress problems soon after sunset.

Key temperature records and occurrence times were summarized in Table 4. Maximum temperatures occurred in the afternoon, and as early as 1300 h at both turf surfaces (Table 4a). At NT, the maximum temperature decreased with height. At AT, maximum temperature of turf surface was the same as substrate. Maximum temperatures of AT exceeded NT by 32.5 °C and 36.5 °C respectively at turf surface and substrate, whereas air temperatures were higher by 6.5 °C at 15 cm, 2.3 °C at 50 cm, and similar at 150 cm. The two sites had similar minimum temperatures, except substrate with AT warmer than NT by 3.4 °C (Table 4b).

The AT diurnal temperature range reached 50.7 °C at turf surface and 45.4 °C at substrate, exceeding NT by 36.5 °C and 35.9 °C (Table 4c). The differences shrank to 6.5 °C at 15 cm, 2.4 °C at 50 cm, and merely 0.7 °C at 150 cm. The ATI had the largest difference between the two sites at turf surface (28.8) and substrate (24.7). They were notable lower for air temperatures (Table 4d). Site ATI of AT was very high at 17.80 vis-à-vis NT with only 5.42. The thermal ambience to players was notably more stressful at AT. AT materials were warmed well above NT's due to a combination of inherent and predisposing factors, including low albedo, low specific heat of the plastic fibers (Professional Plastics, 2015) and rubber-granule infill materials (Nah, Park, Cho, Chang, & Kaang, 1999), and low moisture content which suppresses the substrate thermal capacity. More solar radiation absorbed by AT turf surface was transformed to sensible heat. With limited thermal capacity, solar radiation can notably raise material temperature at a fast rate with hardly any time lag. With little moisture in the emulated grass-leaf fibers and infill materials, evaporative cooling was restricted and little heat could be stored in feeding the thermal-mass effect. The heated materials in turn can emit longwave ground radiation to increase the radiation load. The limited thermal storage is a two-edged sword, as it could also allow relatively fast cooling. The intense radiant-energy regime in tropical sunny daytime could present acute heat stress to athletes (Larsen et al., 2007). Approaching and soon after sunset, however, AT turf surface and substrate could cool down rather quickly to dampen the heat-stress risk.

In contrast, NT had higher albedo, higher specific heat of grass tissues, and mineral soil with porosity partly filled by water to raise specific heat (Abu-hamdeh, 2003). These compositions and properties fostered evapotranspiration to bring latent heat cooling (Jayalakshmy and Philip, 2010) and imparted a higher thermal capacity to retard the rate and range of temperature rise and fall. Therefore, NT could not heat up to a high level, and would warm up and cool down at a relatively slower pace.

3.6. Temperature profile on cloudy day

The reduced solar radiation input brought notable temperature responses at both sites (Fig. 8). At 0800 h, the two curves nearly overlap except turf surface which was already warmer at AT by 5.6 °C (Fig. 8a). The NT turf surface was able to cool overnight with the help of evaporation to 26.7 °C, the lowest of the five levels, to create a small temperature inversion near the ground. The dry AT materials could not benefit from evaporative cooling at night. The feeble solar energy in early morning began to initiate mild warming at AT. In nighttime, ground thermal radiation loss was only slightly higher than sky thermal radiation gain, hence its overnight cooling effect at turf surface and substrate was limited.

At 1000 h, the morning solar radiation input managed to trigger warming at AT turf surface and substrate, quickly pushing the temperatures respectively by 11.5 °C and 9.5 °C above NT (Fig. 8b). Air temperature at 15 cm was raised by 1.3 °C, but higher up the warming effect did not bring notable differences between the two sites. The NT turf surface remained cooler than other elevations to sustain the ground-hugging temperature inversion. At noon, AT temperatures climbed quickly to 52.7 °C at turf surface and 54.2 °C at substrate. They were close to the maximum of the day, departing notably from 150-cm air temperature at 31.1 °C (Fig. 8c). The maximum temperature of 65.8 °C was reached at 1130 h (Table 4). Meanwhile, NT temperatures stayed relatively low, reaching 33.0 °C at turf surface and 35.1 °C at substrate. This is the only time when the near-ground temperature inversion was suppressed. Warming due to solar irradiance was more or less nullified by evapotranspiration cooling to maintain a relatively cool turf surface and substrate. Nevertheless, the rate of evapotranspiration cooling was not adequate to retain the temperature inversion at turf surface. The intensity of insolation on the cloudy day, even at noontime, was unable to exceed the *energy balance tipping-point* (EBT) between the two opposing forces of warming vis-à-vis cooling. At AT, the lower albedo, more incident insolation and lack of latent heat dissipation jointly raised turf surface and substrate temperatures. The maximum temperature of the day was reached around noon to synchronize with maximum solar radiation input.

At 1400 h, with decline in direct solar radiation input, the two sites expressed different responses (Fig. 8d). At NT, the temperature inversion at the turf surface was re-established at 26.7 °C, reflecting that the energy budget has dropped further below the EBT. Meanwhile, soil moisture in the substrate was able to nurture the thermal mass and raise its temperature to 35.7 °C. At AT, the reduced insolation brought fast drop in turf surface temperature to 38.3 °C. The substrate temperature dropped but was kept at 47.6 °C due to thermal inertia.

At 1600 h and 1800 h, the solar radiation input subsided, and the turf surface and substrate temperatures at both sites dropped down to several degrees above air at 150 cm (Fig. 8e and f). NT turf surface continued to sustain the small temperature inversion. The AT temperature at turf surface (respectively 35.0 °C and 31.2 °C) stayed at 5–6 °C above NT, and at 15 cm 1–2 °C above NT. For sports turf use, from 1600 h onwards, the heat stress at AT was not notably higher than NT. It signified that on summer cloudy days from mid-afternoon onwards, AT could lapse into a relatively *heat-safe period* for players. This finding hints that games could be scheduled to avoid the hottest periods, and they could be shifted to times and weather conditions with relatively lower temperature (Grundstein et al., 2014; Kajiwara et al., 2005). The summer cloudy day offers a wider window to meet such demands.

For maximum temperature, despite the reduced solar radiation input, AT still exceeded NT by 29.7 °C at turf surface and 22.5 °C at

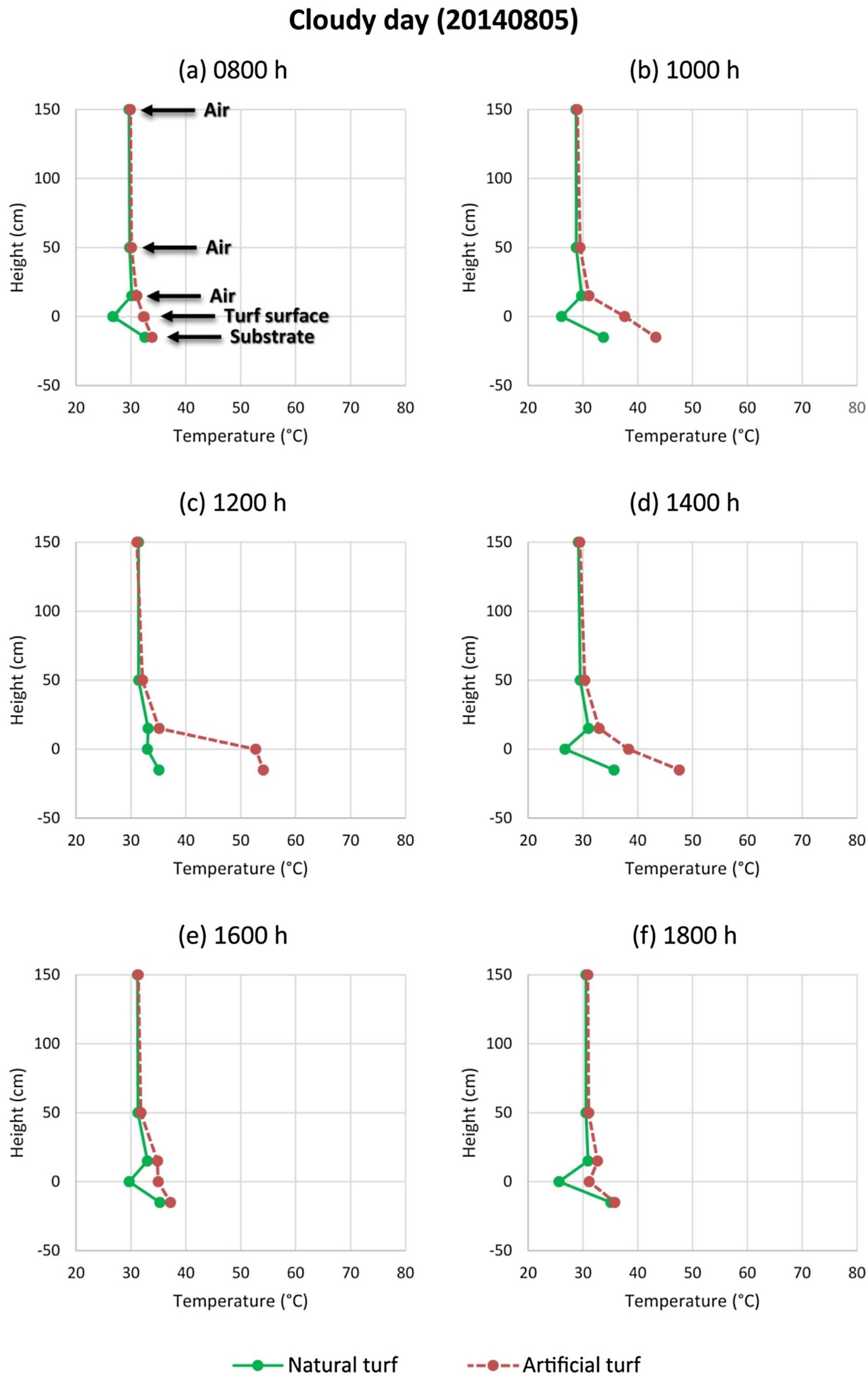

Fig. 8. Vertical temperature profiles from 150 cm height to substrate at six times on the cloudy day (CD) comparing natural and artificial turf sites.

Table 4
Selected temperature records at the natural and artificial turf sites respectively on sunny, cloudy and overcast sampled days.

Temperature attribute	Natural turf (NT)			Artificial turf (AT)			AT − NT[c]		
	Sunny 20140705	Cloudy 20140805	Overcast 20140707	Sunny 20140705	Cloudy 20140805	Overcast 20140707	Sunny 20140705	Cloudy 20140805	Overcast 20140707
(a) Maximum temperature:									
Air at 150 cm (°C)	34.4	32.3	30.5	34.4	33.6	32.4	−0.1	1.3	1.9
Occurrence time (h)	1630	1330	0645	1500	1130	1100	−0130	−0200	0415
Air at 50 cm (°C)	34.6	32.4	31.0	36.9	34.7	33.5	2.3	2.3	2.6
Occurrence time (h)	1400	1330	1100	1500	1130	1100	0100	−0200	0000
Air at 15 cm (°C)	37.6	34.7	32.4	44.1	38.4	37.8	6.5	3.8	5.4
Occurrence time (h)	1545	1330	1100	1400	1130	1100	−0145	−0200	0000
Turf surface (°C)	37.3	36.1	31.6	73.8	65.8	52.5	36.5	29.7	20.9
Occurrence time (h)	1315	1130	1100	1300	1130	1100	−0015	0000	0000
Substrate at 6 mm depth (°C)	41.4	35.7	34.6	73.8	58.2	49.6	32.5	22.5	15.0
Occurrence time (h)	1515	1400	1130	1315	1145	1115	−0200	−0215	−0015
(b) Minimum temperature:									
Air at 150 cm (°C)	28.3	28.2	27.7	29.0	28.2	28.1	0.6	−0.1	0.4
Occurrence time (h)	0915	0500	0930	0400	0230	1200	−0515	−0230	0230
Air at 50 cm (°C)	28.8	28.0	27.9	28.7	27.9	27.9	0.0	−0.1	0.0
Occurrence time (h)	0400	0315	2315	0400	0415	2315	0000	0100	0000
Air at 15 cm (°C)	28.3	27.5	27.5	28.2	27.6	27.4	0.0	0.1	−0.1
Occurrence time (h)	0415	0415	2315	0415	0415	2315	0000	0000	0000
Turf surface (°C)	23.2	22.0	22.7	23.2	22.8	23.1	0.0	0.7	0.4
Occurrence time (h)	0415	0415	2345	0415	0415	2315	0000	0000	−0030
Substrate at 6 mm depth (°C)	31.8	32.5	31.3	28.4	28.2	27.5	−3.4	−4.2	−3.7
Occurrence time (h)	0700	0715	2345	0430	0430	2330	−0230	−0245	−0015
(c) Diurnal temperature range:									
Air at 150 cm (°C)	6.12	4.06	2.79	5.40	5.43	4.28	−0.7	1.4	1.5
Air at 50 cm (°C)	5.83	4.44	3.08	8.19	6.83	5.67	2.4	2.4	2.6
Air at 15 cm (°C)	9.38	7.17	4.90	15.86	10.87	10.43	6.5	3.7	5.5
Turf surface (°C)	14.15	14.10	8.92	50.70	43.05	29.41	36.5	28.9	20.5
Substrate at 6 mm depth (°C)	9.55	3.25	3.38	45.40	30.00	22.07	35.9	26.8	18.7
(d) Aggregate thermal index (ATI)[a]:									
Air at 150 cm (°C)	3.29	1.03	−0.21	3.56	1.25	0.27	0.3	0.2	0.5
Air at 50 cm (°C)	3.54	1.14	−0.14	5.61	1.83	0.51	2.1	0.7	0.6
Air at 15 cm (°C)	5.53	2.31	−0.02	11.57	4.51	1.59	6.0	2.2	1.6
Turf surface (°C)	4.97	0.32	−3.34	33.78	13.66	3.68	28.8	13.3	7.0
Substrate at 6 mm depth (°C)	9.78	5.23	3.80	34.48	14.93	6.70	24.7	9.7	2.9
Site ATI[b]	5.42	2.01	0.02	17.80	7.24	2.55	12.4	5.2	2.5

[a] Using the top 32 values of the sampled day and 30 °C as threshold temperature, $ATI = \Sigma(x - 30)/32$.
[b] Site ATI is the average of the five ATI values at individual measurement positions.
[c] The difference in timing (AT-NT) is expressed as hhmm, e.g. 0545 means AT 5 h 45 min ahead of NT, and −0545 mean behind.

substrate (Table 4a). The inherent difference in thermal properties and behaviors of the two turf sites sustained a wide divergence in mainly material temperatures. For minimum temperature, the two sites were similar except at substrate where NT was warmer than AT by 4.2 °C (Table 4b). This result verified the existence of thermal mass and hence thermal inertia at NT substrate due to presence of water with high specific heat.

The diurnal temperature ranges at AT were considerably higher than NT (Table 4c). Reduction in solar radiation input, however, had suppressed the inter-site differences to 28.9 °C at turf surface and 26.8 °C at substrate. ATI values were considerably depressed on cloudy day, and the differences between AT and NT had been reduced to around 10 at the turf surface and substrate (Table 4d). Site ATI was depressed considerably to 7.24 at AT in comparison with 2.01 at NT.

3.7. Temperature profile on overcast day

On overcast day, direct solar radiation peaked at 1100 h, and dropped to only about 40–60 W m^{-2} thereafter. The 7 mm of rainfall happened around 1100 h to reduce heat accumulation towards noontime. The temperature profiles faithfully reflected this radiant energy pattern (Fig. 9). At 0800 h, the two sites had similar temperature patterns except lingering of turf surface temperature inversion at NT (Fig. 9a). Notable warming of turf surface and substrate occurred only at 1000 h at AT, lifting temperatures respectively to 41.3 °C and 42.6 °C (Fig. 9b). Despite the much subdued solar radiation input, AT air temperatures at 150 cm, 50 cm and 15 cm were all warmed to about 2–4 °C above NT. In the remainder of the day, the temperature curves of the two sites nearly converged even at noon (Fig. 9c–f). Both fields would not incur excessive heat stress for players on the overcast day.

Despite the weak solar radiation input, the overcast day maintained a rather high maximum temperature at AT of 52.5 °C at turf surface and 49.6 °C at substrate (Table 4a). The small amount of sunshine was able to heat up AT materials. In contrast, at NT the material maximum temperatures were only a few degrees above 150-cm value. High specific heat of grass tissues and soil could resist temperature rise and compress diurnal temperature amplitude under the low solar-radiation regime. For minimum temperature, NT and AT were similar except that NT substrate was warmer by 3.7 °C (Table 4b).

The diurnal temperature range of AT exceeded NT at all measurement levels (Table 4c). Despite the feeble solar irradiance, AT turf surface and substrate were respectively 20.5 °C and 18.7 °C higher than NT. The differences were due to higher AT maximum rather than lower minimum. Both sites experienced significant drop in ATI, being more so at NT (Table 4d). Site ATI at NT dropped down to merely 0.02 whereas AT sustained 2.55.

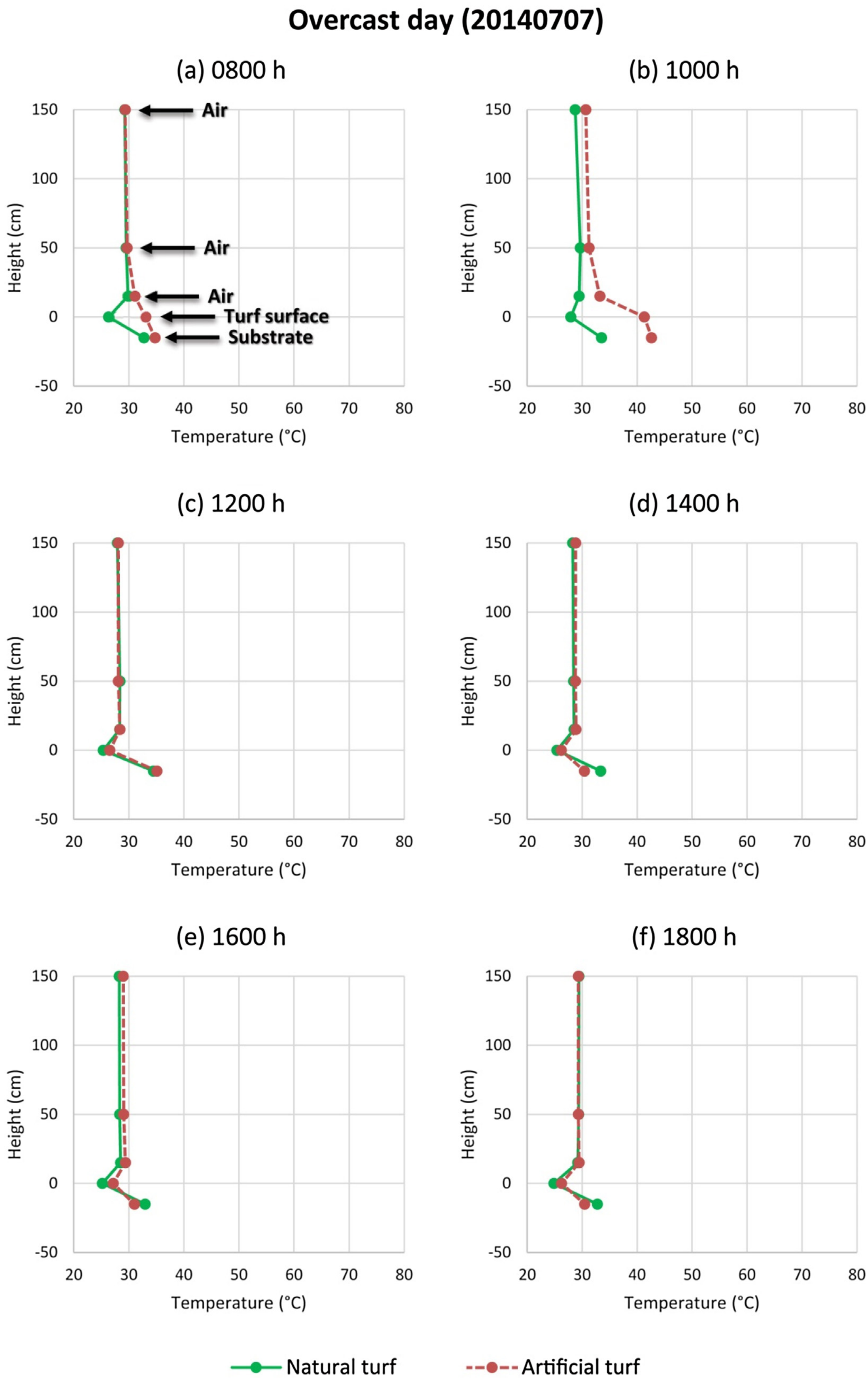

Fig. 9. Vertical temperature profiles from 150 cm height to substrate at six times on the overcast day (OD) comparing natural and artificial turf sites.

4. General discussion and conclusion

Partitioning the multiple energy pathways at the turf sites could ascertain the radiant and sensible-heat energy budgets with important bearing on their thermal regimes. Solar radiation in the tropical summer is dominated by strong incoming irradiance with a small outgoing (reflected) portion. Cloudy day considerably attenuates solar radiation input to about half, and overcast day about a quarter. Terrestrial radiation, on the other hand, has sizeable sky thermal radiation influx as well as ground thermal radiation efflux components, occurring continually in both daytime and nighttime. They are less affected by weather conditions in the absence of rainfall. Despite drastic reduction in solar gain from sunny to cloudy and overcast days, incoming and outgoing terrestrial radiation in daytime and nighttime are sustained at a high level. By total energy flux on a daily basis, a considerably larger amount of thermal radiant energy than solar energy is fluxed in the near-ground ambience of the turf sites.

The two components of the radiant energy budget offer the crucial determinants of NT and AT thermal performance. For shortwave radiation, AT has a lower solar reflectance than NT to increase its solar gain. The differential is maintained in relative terms regardless of weather condition. For longwave radiation, AT has higher ground thermal or terrestrial re-radiation than NT to increase its thermal loss and hence thermal load on players. The sunny day has the highest ground thermal emission, followed by cloudy and overcast. AT absorbs more solar radiation and releases more thermal radiation to generate a high energy-content ambience. AT in effect serves as an efficient processor of solar energy, receiving more, converting promptly more to sensible heat, and shifting more heat to the near-ground environment. The relative proportions of the main radiant energy components play key roles in the divergent thermal expression of the two turf sites.

The total radiant flux index (RFI) presents an aggregate quantitative measure of the amount of radiant energy passing through the fields. The RFI of the three weather days is on average 100:87:80 (sunny:cloudy:overcast), indicating progressive reduction in radiant flux contents (Table 3). In comparison, the corresponding net radiation is on average 100:50:20. The discrepancies between these two numerical sequences imply that despite the drastic curtailment of insolation, terrestrial radiation fluxes continue to operate intensely to support relatively high RFI values. For a given weather day, the two turf sites have similar RFI as well as net radiation values. It implies that NT admits less radiant energy and emits less; AT admits more and emits more. This finding signifies the fundamental basis of the differential thermal behavior of the two fields.

In contrast, the relative contributions of solar and terrestrial radiation, measured by radiant flux ratio (RFR), differ greatly between the weather days (Table 3). For NT, it ranges from 0.36 (sunny) to 0.20 (cloudy) and 0.10 (overcast). For AT, the respective values are consistently lower at 0.30, 0.17 and 0.08. The results signify substantial increase in terrestrial radiation components along the weather sequence. The consistently lower RFR of AT than NT indicates that greater terrestrial components are conducive to material and air warming. Ground thermal radiation is higher than sky thermal radiation for all weather days. It indicates the importance of outgoing infrared radiation in tandem with conduction and convection in releasing AT stored sensible heat. Moreover, the ground thermal radiation at AT is higher than NT on days with more solar radiation inputs (sunny and cloudy), but it is similar on overcast day. Thus strong insolation is necessary to drive more ground thermal emission at AT than NT to accentuate inter-site divergence in thermal regimes. This phenomenon could be labelled *solar-induced thermal divergence*, which diminishes in effect with decline in insolation.

Acquiring more solar radiation due to lower albedo presents the predisposing and necessary but not sufficient condition to induce drastic rise in AT material (turf surface and substrate) temperature. The thermal properties and behaviors of AT materials substantially account for the heat absorption, retention, transmission, emission and release. The plastic imitation grass blades (piles) and the black rubber granules (infill) have low specific heat and little moisture-holding capacity. Upon absorbing solar energy, they are quickly heated up with little time lag, bringing unusually high maximum temperature and wide diurnal temperature amplitude. In contrast, NT with higher specific heat and moisture content to sustain evapotranspiration cooling, suppresses warming, creates thermal mass effect, generates thermal inertia, delays warming, but also postpones cooling. Thus NT has notably lower maximum temperature and narrower diurnal temperature amplitude.

The sunny day heats AT materials to over 70 °C, attained at noontime and maintained in the early afternoon. The retained heat is in turn transferred to near-ground air by conduction and convection to raise air temperature to above 40 °C. In turn, the heated surface emits a large quantity of infrared radiation. The AT site is immersed in an ambience of intense radiant fluxes composing of direct solar radiation, incoming and outgoing infrared radiation, as well as strong sensible-heat streams emanating from the hot AT material. Their joint impact on athletes can induce heat stress to exceed the safety threshold and harm their health and performance. The daytime period is particularly heat-risky and should be avoided for games and practices.

On sunny day, the confined heat reservoir at the AT field, however, demonstrates an easy-come-easy-go phenomenon. Fast warming in the early part of the day is accompanied by fast cooling in late afternoon. High emissivity in the infrared spectrum feeds efficient heat dissipation by ground thermal radiation, thus allowing relatively safe use by players soon after sunset. In contrast, NT suppresses and delays warming, postpones cooling, and extends gentle warming over a longer period. The maximum temperature at the NT turf surface stays in the thirties, which is only a few degrees above the 150-cm ambient air temperature. The effective latent heat dispersion by evapotranspiration at NT creates a small temperature inversion near the turf surface outside the hottest period around noontime.

On cloudy day, solar irradiance is drastically curtailed, but thermal radiation components do not experience a corresponding decline. The AT turf surface can still be heated to the maximum of 65.8 °C shortly before noon. Part of the stored heat is transferred to near-ground air, warming it to about 5 °C degrees higher than the 150-cm level. In daytime, ground thermal emission still exceeds sky thermal. A notable amount of infrared radiation is emitted by the hot ground at a lower quantity than sunny day. From 1600 h, the subsidence in insolation induces prompt cooling to dampen turf surface temperature. At 1800 h the turf surface temperature drops down to 31.2 °C which is not notably warmer than NT. Overall, summer cloudy day is still too hot from late morning to late afternoon for sports events. However, it could cool down to an acceptable level from late afternoon onwards. Games and practices should avoid the hottest circum-midday periods and be accommodated in the wider heat-safe window.

The overcast day notably depresses solar radiation input and brings small collateral reduction in terrestrial radiant fluxes. Sky thermal and ground thermal radiation components still remain rather high which are comparable to cloudy day. The inter-site differential in terms of sky thermal and ground thermal radiation components shrinks notably. AT still emits more infrared radiation than NT, and it sustains a higher maximum temperature above 50 °C for a short period. For most of the day, the two fields are similar in terms of human thermal comfort to players, thus offering flexibility to schedule matches or practices. The findings clarify the regulation of the thermal regimes at natural and artificial turf fields by solar and terrestrial radiant energy fluxes under different weather conditions in summer. The changes in radiation and temperature in the diurnal cycle, and the relationships between the two attributes, have been ascertained by the detailed field-experiment data. The analysis can improve understanding of the complex relationships amongst the key factors and the associated processes leading to the inordinate temperature elevation at AT sites. The daily marches of radiation and temperature provide an objective basis to identify the heat-safe windows and to optimize scheduling of events to avoid heat-stress health impacts.

Acknowledgments

The research grants kindly furnished by the Dr Stanley Ho Alumni Challenge Fund and the University Grants Committee Matching Fund are grateful acknowledged. The permission to conduct the field experiments at my university's sports fields is warmly appreciated. Thanks are extended to Jeannette Liu and W.Y. Wong for their field assistance.

References

Abu-hamdeh, N. H. (2003). Thermal properties of soils as affected by density and water content. *Biosystems Engineering*, *86*, 97–102.
Amengual, A., Homar, V., Romero, R., Brooks, H. E., Ramis, C., Gordaliza, M., et al. (2014). Projections of heat waves with high impact on human health in Europe. *Global and Planetary Change*, *119*, 71–84.
Aoki, T., Matsuda, T., & Toyoda, K. (2005). Sport environments for children: focusing on surface layer temperature of artificial turf. *Bulletin of Biwako Sekei Sport College*, *2*, 93–98.
Aoki, T. (2011). *Current state and perspective for artificial turf as sport environment: Focusing on third-generation artificial turf as footfall playing surface*. Osaka, Japan: Biwako Seikei Sport College., 19pp.
Brakeman, L. (2004). *Infill system spark debate at STMA Conference*.. http://www.athleticturf.net/athleticturf/article/articleDetail.jsp?id=85955 Accessed 12.09.15
Buskirk, E. R., Mclaughlin, E. R., & Loomis, J. L. (1971). Microclimate over artificial turf. *Journal of Health, Physical Education, Recreation*, *42*, 29–30.
Chong, S. N., & Lee, T. C. (2015). *Solar energy resources in Hong Kong from a climatological point of view*. Hong Kong: Hong Kong Observatory.
Claudio, L. (2008). Synthetic turf: Health debate takes root. *Environmental Health Perspectives*, *116*, 116–122.
Department of Sport and Recreation. (2011). *Natural Grass v Synthetic Turf Study Report*. Perth: Department of Sport and Recreation, Government of Western Australia.
FIFA. (2015). *FIFA quality concept for football turf*. Zurich, Switzerland: International Federation of Football Associations. http://www.FIFA.com/en/development/quality/index.html Accessed 12.10.15
FIH. (2014). *Handbook of performance, durability and construction requirements for synthetic turf hockey pitches*. Lausanne, Switzerland: International Hockey Federation., http://www.FIFA.com/en/development/quality/index.html Accessed 12.10.15.
Fleming, P. (2011). Artificial turf systems for sport surfaces: Current knowledge and research needs. *Proceedings Institute of Mechanical Engineering 225 Part P: Journal of Sports Engineering and Technology*, *225*, 43–63.
Fresenburg, B. (2005). *Synthetic turf playing fields present unique dangers*. Columbia, MO: Plant Management Network, University of Missouri.
Gates, D. M. (2003). *Biophysical ecology*. Mineola, NY: Dover.
Grundstein, A., Cooper, E., Ferrara, M., & Knox, J. A. (2014). The geography of extreme heat hazards for American football players. *Applied Geography*, *46*, 53–60.
Hong Kong Council of Social Service. (2014). *Social indicators of Hong Kong: Per capita area of public open space. Hong Kong*.. http://www.socialindicators.org.hk/en/indicators/environmental_quality Accessed 22.09.15
Hong Kong Observatory. (2015a). *Monthly meteorological normal for Hong Kong*. Hong Kong: Hong Kong Observatory.
Hong Kong Observatory. (2015b). *Observed climate change in Hong Kong*. Hong Kong: Hong Kong Observatory.
Hong Kong Observatory. (2016). *1981-2010 monthly meteorological normal for Hong Kong*. Hong Kong: Hong Kong Observatory.
Howe, A. S., & Boden, B. P. (2007). Heat-related illness in athletes. *American Journal of Sports Medicine*, *35*, 1384–1395.
IPCC. (2013). Summary for policymakers. In T. F. Stocker, D. Qin, G.-K. Plattner, M. Tignor, S. K. Allen, J. Boschung, A. Nauels, Y. Xia, V. Bex, & P. M. Midgley (Eds.), *Climate change 2013: The physical science basis. Contribution of Working Group I to the Fifth Assessment Report of the Intergovernmental Panel on Climate Change*. http://www.climatechange2013.org/images/uploads/WGI_AR5_SPMbrochure.pdf Accessed 12.10.15
Jayalakshmy, M. S., & Philip, J. (2010). Thermophysical properties of plant leaves and their influence on the environment temperature. *International Journal of Thermophysics*, *31*, 2259–2304.
Jim, C. Y., & Chan, M. W. H. (2016). Urban greenspace delivery in Hong Kong: Spatial-institutional limitations and solutions. *Urban Forestry and Urban Greening*, *18*, 65–85.
Jim, C. Y. (1996). Edaphic properties and horticultural applications of some common growing media. *Communications in Soil Science and Plant Analysis*, *27*, 2049–2064.
Jim, C. Y. (2015). Assessing climate-adaptation effect of extensive tropical green roofs in cities. *Landscape and Urban Planning*, *138*, 54–70.
Kajiwara, Y., Ono, S., Nakai, S., Kimura, K., & Nozaki, T. (2005). Environmental temperature during summertime athletic competitions in Japan. In Y. Tochihara, & T. Ohnaka (Eds.), *Environmental ergonomics* (pp. 71–77). Amsterdam: Elsevier.
Kandelin, W. W., Krahenbuhl, G. S., & Schacht, C. A. (1976). Athletic field microclimates and heat stress. *Journal of Safety Research*, *8*, 106–111.
Kipp and Zonen. (2009). *CNR 4 Net Radiometer Instruction Manual*. The Netherlands: Kipp & Zonen., 35 pp.
Larsen, T., Kumar, S., Grimmer, K., Potter, A., Farquharson, T., & Sharpe, P. (2007). A systematic review of guidelines for the prevention of heat illness in community-based sports participants and officials. *Journal of Science and Medicine in Sport*, *10*, 11–26.
Lee, T. C., Chan, H. S., Ginn, E. W. L., & Wong, M. C. (2011). Long-term trends in extreme temperatures in Hong Kong and southern China. *Advances in Atmospheric Sciences*, *28*, 147–157.
Lo, A. Y., & Jim, C. Y. (2015). Come rain or shine? Public expectation on local weather change and differential effects on climate change attitude. *Public Understanding of Science*, *24*, 928–942.
Madison Athletic Foundation. (2011). *The facts about SBR: Tire rubber used in artificial turf fields*. Madison, NJ: Madison Athletic Foundation.
McNitt, A. S., & Petrunak, D. M. (2007). *Evaluation of playing surface characteristics of various in-filled systems*. Pennsylvania State University, Plant Science Extension. http://plantscience.psu.edu/research/centers/turf/extension/factsheets/playing-surfaces Accessed 28.08.16
McNitt, A. S. (2005). Synthetic turf in the USA: Trends and issues. *International Turfgrass Society Research Journal*, *10*, 27–33.
Nah, C. W., Park, J. H., Cho, C. T., Chang, Y. W., & Kaang, S. Y. (1999). Specific heats of rubber compounds. *Journal of Applied Polymer Science*, *72*, 1513–1522.
Petrass, L. A., Twomey, D. M., & Harvey, J. T. (2014). Understanding how the components of a synthetic turf system contribute to increased surface temperature. *Procedia Engineering*, *72*, 943–948.
Petrass, L. A., Twomey, D. M., Harvey, J. T., Otago, L., & LeRossignol, P. (2015). Comparison of surface temperatures of different synthetic turf systems and natural grass: Have advances in synthetic turf technology made a difference. *Journal of Sports Engineering and Technology*, *229*, 10–16.
Planning Department. (2015). *Planning statistics: Land utilization in Hong Kong*. Hong Kong: Hong Kong Government. http://www.pland.gov.hk/pland_en/info_serv/statistic/landu.html Accessed on 15.09.15
Professional Plastics. (2015). *Thermal properties of plastic materials. Fullerton, CA*.. http://www.professionalplastics.com/professionalplastics/ThermalPropertiesofPlasticMaterials.pdf Accessed 20.10.15
Ramsey, J. D. (1982). Environmental heat from synthetic and natural turf. *Research Quarterly for Exercise and Sport*, *53*, 82–85.
Sciacca, T. (2008). *The thermal physics of artificial turf*.. http://www.synturf.org/sciaccaheatstudy.html Accessed 28.08.16
Williams, F. C., & Pulley, G. E. (2002). *Synthetic surface heat studies*. Brigham Young University. http://cahe.nmsu.edu/programs/turf/documents/brigham-young-study.pdf Accessed 28.08.16